

# Preliminary comparisons of the typical polarized radiative transfer models: precision and efficiency

GAO Yang<sup>1</sup>, DUAN Minzheng<sup>2</sup>, HUANG Xingyou<sup>1</sup>

1. School of Atmospheric Physics, Nanjing University of Information Science & Technology, Jiangsu Nanjing 210044, China;

2. Institute of Atmospheric Physics, Chinese Academy of Sciences, Beijing 100029, China

**Abstract:** Radiative transfer models are key tools in the remote sensing and parameterization of climate radiative forcing, while polarized radiative transfer models can provide more accurate insights into the radiation processes in the earth-atmosphere system. PolRadtran/RT3 (Polarized Radiative Transfer, based on the adding-doubling method), SOSVRT (Vector Radiative Transfer, based on successive order of scattering), and VDISORT (Vector DIScrete Ordinate Radiative Transfer, a polarized version of DISORT based on the inverse of matrix method), are three of the most common radiative transfer models, each with polarization based on different physical principles. A comparison of their accuracy and efficiency reveals that SOSVRT is the most efficient, with the time consumed remaining almost invariable with the increase of stream numbers, but increasing with the optical depth of the layered atmosphere. For example, the time consumed for an optical depth of 1.0 was found to be two times that for an optical depth of 0.5 for the Mie scattering atmosphere. The efficiencies of RT3 and VDISORT in modeling polarization with a large stream number were found to be low. For example, under the Rayleigh scattering atmosphere at 400nm and a stream number of 40, the time consumed was 23 times and 7 times as much as that of SOSVRT, respectively. The computation time for the two models was found not to be sensitive to the optical depth, but increased greatly with the increase in stream number. All three models were found to be of the same order of accuracy, but VDISORT showed a fluctuating result for simulations with large streams.

**Key words:** polarized radiative transfer, adding-doubling method, successive order of scattering, DISORT

**CLC number:** TP701      **Document code:** A

**Citation format:** Gao Y, Duan M Z and Huang X Y. 2010. Preliminary comparisons of the typical polarized radiative transfer models: precision and efficiency. *Journal of Remote Sensing*. 14(5): 839—851

## 1 INTRODUCTION

Measurements and simulation of the transfer processes of radiation in the atmosphere are two of the most important aspects in remote sensing. Both the intensity of the radiation and its state of polarization should be taken into account in radiative transfer simulations. If polarization is neglected, one can expect an error level of around 10% to be introduced (Chandrasekhar, 1950). A scalar radiative transfer model cannot completely describe the nature of the radiation processes and it is not exact enough for studies where a high level of accuracy is needed. Under clear sky conditions, scalar radiative transfer modeling can produce 5%–10% error in intensity readings (Lacis *et al.*, 1998). Stam and Hovenier (2005) pointed out that error of 10% or even more can be induced in the derivation of the gas mixing ratio and the shape of aerosol due to neglecting polarization in the simulation of radiative transfer.

A polarized signal can be used to separate the contributions of the atmosphere and the surface (Deuzé *et al.*, 1993; Duan & Lu, 2007, 2008), as well as provide useful information on the

shape of particles and cloud phase. More and more instruments with the ability to monitor polarization are being deployed in atmospheric and astronomical research, such as CIMEL, POLDER/ADEOS and its successor PARASOL, and the Aerosol Polarimetry Sensor (APS), which will be onboard the GLORY satellite to be launched in 2010. However, if there is no reliable vector radiative transfer model, polarization measurements cannot be used to derive accurate information of the Earth's atmosphere and surface. The absolute magnitude of polarization, especially the component V, which is in the order of  $10^{-4}$  to  $10^{-5}$ , is relatively small, and so the vector radiative transfer model with its high degree of accuracy is required. A radiative transfer model with polarization can be used to interpret radiative processes more accurately compared with a scalar model, but the computing time is much longer, and a fast and accurate polarized radiative transfer model is required in the inversion algorithm. PolRadtran/RT3 (Polarized Radiative Transfer, RT3 for short, based on the adding-doubling method (Evans, 1991), VDISORT, a vector version of DISORT (DIScrete Ordinate Radiative Transfer) developed by Schulz *et al.*

**Received:** 2009-11-10; **Accepted:** 2010-04-28

**Foundation:** High Technology Research and Development Program of China (No. 2009AA12Z151), National Basic Research Program of China (No. 2006CB403702) and the National Basic Research Program of China (No. 2006CD403707).

**First author biography:** GAO Yang (1985— ), male, graduate student at Nanjing University of Information Science & Technology. His research interests focus on radiative Effects of atmosphere aerosols. E-mail: tony0519@sohu.com

(1999) and SOSVRT (Vector Radiative Transfer, based on successive order of scattering) (Min & Duan, 2004; Duan *et al.*, 2010) are three of the most commonly used models.

## 2 VECTOR RADIATIVE TRANSFER EQUATION

The energy radiation and the state of the polarization can be described by the Stokes vector  $\mathbf{I}=[I, Q, U, V]^T$ , where  $I$  denotes the intensity of the radiation;  $Q$  the type of the vector endpoint trajectory of the radiation field;  $U$  the orientation of the ellipse major axis;  $V$  the direction of rotation of the polarization vector end (McLinden *et al.*, 2002); and the superscript T denotes the transpose symbol. The propagation and distribution of the Stokes vector in a plain-parallel medium with scattering and absorption can be expressed as:

$$\mu \frac{d\mathbf{I}(\tau, \mu, \phi)}{d\tau} = -\mathbf{I}(\tau, \mu, \phi) + \mathbf{J}(\tau, \mu, \phi) \quad (1)$$

The scalar radiative transfer equation has an identical form by replacing vector  $\mathbf{I}$  with  $I$ .  $\mathbf{J}(\tau, \mu, \phi)$  in the above equation is the source function, which can be expressed as:

$$\mathbf{J}(\tau, \mu, \phi) = \frac{\omega}{4\pi} \int_0^{2\pi} \int_{-1}^1 \mathbf{M}(\tau, \mu, \phi; \mu', \phi') \mathbf{I}(\tau, \mu', \phi') d\mu' d\phi' + \frac{\omega}{4\pi} \mathbf{F}_0 \exp(-\tau/\mu_0) \mathbf{M}(\tau, \mu, \phi; -\mu_0, \phi_0) \quad (2)$$

$$\mathbf{I} = \sum_{m=0}^M [I_m \cos m(\phi - \phi_0), Q_m \cos m(\phi - \phi_0), U_m \sin m(\phi - \phi_0), V_m \sin m(\phi - \phi_0)]^T \quad (6)$$

$$\mathbf{M} = \frac{1}{2} \mathbf{C}_0 + \sum_{m=1}^M [C_m \cos m(\phi - \phi') + S_m \sin m(\phi - \phi')] \quad (7)$$

where  $C_m$  and  $S_m$  are the coefficients of the  $m^{\text{th}}$  Fourier mode. By inserting Eq. (6) and Eq. (7) into Eq. (1), we have the radiative transfer equation for each Fourier mode (Duan *et al.*, 2010):

$$\mu \frac{d\mathbf{I}_m(\tau, \mu)}{d\tau} = -\mathbf{I}_m(\tau, \mu) + \mathbf{J}_m(\tau, \mu) \quad (8)$$

$\mathbf{J}_m$  can be described as:

$$\mathbf{J}_m(\tau, \mu) = \frac{\omega}{4} \int_{-1}^1 \mathbf{M}_m(\tau, \mu; \mu') \mathbf{I}_m(\tau, \mu) d\mu' + \frac{(2 - \delta_{0m}) \omega}{2} \frac{\omega}{4\pi} \exp(-\tau/\mu_0) \mathbf{M}_m(\tau, \mu; -\mu_0) \mathbf{F}_0 \quad (9)$$

In the following sections, based on different discretization of the above equation, different numerical models are obtained, the three most commonly used models are introduced, and their computation efficiencies and accuracies are compared.

### 2.1 Adding-doubling method

The adding-doubling method is a method based on an intuitive physical process, and is used in a plane-parallel, vertically-inhomogeneous scattering atmosphere. The physical principle is: if the reflection and transmission function of two layers are known, the reflection and transmission function for the combination of the two layers can be calculated simply by addition, and by taking the boundary as a single layer, the upward

where  $\mu$  is the cosine of the zenith angle, positive for downward and negative for upward;  $\phi$  is the azimuth angle;  $\tau$  is the optical depth;  $\omega$  is the single-scattering albedo;  $\mathbf{F}_0=[F_0, 0, 0, 0]$ ;  $F_0$  is the extraterrestrial solar incident flux;  $\mu_0$  is the cosine of the solar zenith angle;  $\phi_0$  is the solar azimuth angle; and  $\mathbf{M}$  is the phase matrix (Mueller matrix) of scattering of 4×4 order. The Mueller matrix,  $\mathbf{M}$ , is obtained by rotational transform of the single-scattering phase matrix,  $\mathbf{P}$  (Min & Duan, 2004; Duan *et al.*, 2010):

$$\mathbf{M} = \mathbf{L}(\pi - i_2) \mathbf{P} \mathbf{L}(-i_1) \quad (3)$$

$\mathbf{L}(i)$  is:

$$\mathbf{L}(i) = \begin{bmatrix} 1 & 0 & 0 & 0 \\ 0 & \cos 2i & \sin 2i & 0 \\ 0 & -\sin 2i & \cos 2i & 0 \\ 0 & 0 & 0 & 1 \end{bmatrix} \quad (4)$$

If the particles are spherical or their surface are mirror-symmetry distributed,  $\mathbf{P}$  has the form:

$$\mathbf{P} = \begin{bmatrix} a_1 & b_1 & 0 & 0 \\ b_1 & a_2 & 0 & 0 \\ 0 & 0 & a_3 & b_2 \\ 0 & 0 & -b_2 & a_4 \end{bmatrix} \quad (5)$$

In order to have a simple and stable numerical algorithm,  $\mathbf{I}$  and  $\mathbf{M}$  are usually expanded as the sum of Fourier serials:

stokes vector at the top of atmosphere (TOA) and downward vector at the surface can be easily derived.

In the adding-doubling method, a thick homogeneous layer is often divided into  $2^N$  identical thin sub-layers, then the reflection and transmission function of the whole layer are given by the doubling method, which greatly speeds up the computation. The doubling method applies for homogeneous layers, and the adding method for inhomogeneous layers. In RT3's code, Fourier expansion is used for the azimuthal angle, and the equations are resolved by direct discretization in the zenith angle and optical depth for each Fourier mode. Two types of surfaces were considered: Lambertian and Fresnel. For calculating the multiple-scattering of the atmosphere, the adding-doubling method are stable and easy to understand (Evans & Stephens, 1991).

### 2.2 Successive order of scattering method

The successive order of scattering method (SOS) is one of the most straightforward approximation methods. In the SOS method, the 1, 2, 3, ...,  $n^{\text{th}}$  scattering is calculated and summed up to derive the total scattering radiance (Min & Duan, 2004).

The computational accuracy of the SOS method is affected by the number of vertical stratifications of the atmosphere and the number of streams, and is also related to the level of scattering. If the optical thickness of each layer is small, and the number of streams large enough, the computational accuracy is high, but at the expense of efficiency.

In SOSVRT, a post-processing source function method (PPSF) is introduced to calculate the Stokes vector at arbitrary angles and optical thicknesses, and this method is much more accurate than standard interpolation.

For the strong forward scattering media, the approximation of phase function with low order polynomial series is not accurate, and can result in false fluctuation, but the computation time may be a burden if a high order polynomial serial is used. The  $\delta$ - $M$  method is introduced into the SOSVRT model to improve the computation efficiency and to remove the false oscillations. The  $\delta$ - $M$  method has been proven to be the most efficient way in radiative transfer simulations of strong anisotropic scattering media.

Compared with other methods, the scattering-absorption process can be calculated easily and is physically clear. The SOS method can trace the photons for each scattering event, the inhomogeneous structure of the medium, as well as take into account gaseous absorption processes. In other words, the SOS method is applicable to the inhomogeneous atmosphere. Furthermore, it is very helpful for radiation parameterization in global climate modeling and to develop fast algorithms in remote sensing. The disadvantage of the SOS method is the slow convergence when the single scattering albedo approaches one for large optical thicknesses. However, in most cases, such as aerosol and thin cirrus sky conditions, where the polarization calculation is required, the optical depth is small. In SOSVRT, several techniques are used to improve the efficiency and the computation time can be reduced greatly. The SOSVRT model has many more advantages than the others in terms of calculating atmospheric polarization.

### 2.3 Discrete ordinate method

The discrete ordinate method is the first to discretize the radiative transfer Eq. (8) and Eq. (9), and a group of first-order linear differential equations are formed ( $2n$  equations,  $2n$  being the number of discrete angles), and then the vector transfer equation can be resolved through the eigenvectors and the eigenvalues of the coefficient matrix; that is, it needs to calculate the inversion of matrix. This is the popular two-stream approximation when  $n=1$  (Shi, 2007), for which there is only one direction both in the upward and downward hemispheres. The coefficient matrix will be sparse and with low convergence if  $n$  is large enough, and also the solution is unstable, resulting in false oscillation.

The discrete ordinate method can calculate the interior variation of the reflection and the transmission function within a layer, and therefore it is accurate and efficient in its calculation of intensity and flux of thick scattering media (Weng, 1992), such as aerosol and cloud.

Through this short introduction of the above three models, we make a conclusion here that VDISORT is based on the direct discretization of the radiative transfer equation, while RT3 and SOSVRT are based on the physical principles of photons

traveling in the absorbing and scattering media. The accuracy and speed, the two key factors for model estimations in simulations of polarization of aerosol and cirrus cloud, are greatly affected by the optical depth and streams, which will be used in the models.

## 3 COMPARISON OF RADIATIVE TRANSFER MODELS

As discussed in the above sections, the scattering phase function is expanded as the summation of a series of orthogonal polynomials. In RT3, the phase function is expanded based on Legendre polynomials, and in VDISORT and SOSVRT it is expanded based on general spherical harmonics polynomials; see Hansen and Travis (1974) for further details. The precision and efficiency of the three models are compared for Rayleigh and Mie scattering sky conditions.

### 3.1 Comparison of computation precision

To calculate and compare the precision of the three models, a homogeneous atmosphere with elliptical spheroids with an aspect ratio of 1.999987, refractive index of  $1.53-0.006i$ , a total optical thickness of 1, and a single scattering albedo of 0.973527 are used; details can be found in model 2 of the literature (Wauben & Hovenier, 1992). The cosine of the solar zenith angle is set to be 0.6 and 16 streams in the hemisphere and a black surface are assumed. The results at three azimuth angles ( $0^\circ$ ,  $90^\circ$ , and  $180^\circ$ ) are compared.

Fig. 1– Fig. 3 show the differences between the three models; the benchmark results are from Wauben and Hovenier (1992), which have been proven accurate with seven digits of precision by several models (Siewert, 2000; Duan & Min, 2004; Duan *et al.*, 2008). The horizontal axis is the cosine of the zenith angle, negative for upward radiation at TOA and positive for downward radiation at the surface. As illustrated in Fig. 1– Fig. 3, the results of VDISORT and RT3 show bigger differences, more than 20%, at the zenith( $-1$ ) and nadir( $1$ ), because spline interpolation is used to compute the radiations at angles other than the Gauss grids in the two models. Bigger differences are also shown in the forward scattering directions and less than 1% at other angles. In SOSVRT, an analytical interpolation algorithm by recalculating the source function is used, and therefore there are only small differences, less than 1% for component  $I$ . Most results of  $I$  components from VDISORT are close to the benchmark, with differences of  $<1\%$ , but there are large errors in the anti-solar direction and about a 3% difference at the cosine of zenith angle 0.6. Except for the horizontal direction (the plane parallel model is not applied to a zenith angle greater than  $80^\circ$ ), results of  $(Q, U, V)$  from SOSVRT are close to the benchmark, with differences less than 0.5%; however the results of RT3 and VDISORT oscillate with the zenith angle. VDISORT shows large errors in the calculation  $V$  component, sometimes with a difference of over 100%.

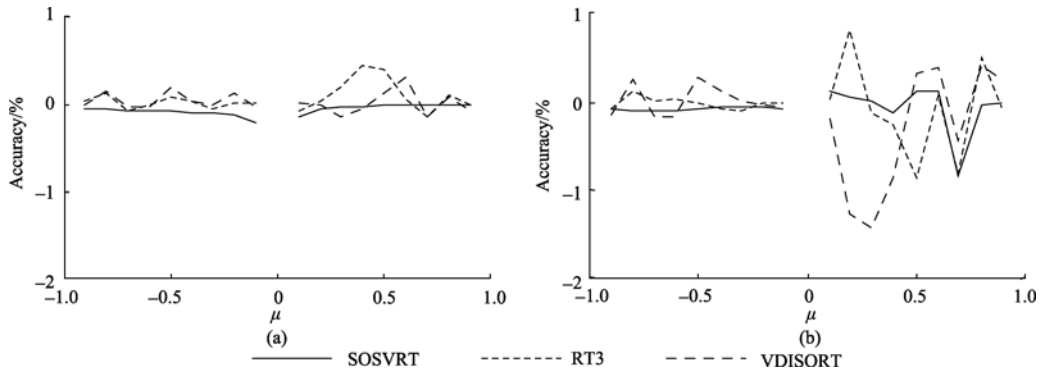


Fig. 1 Error when the azimuth is equal to  $0^\circ$   
(a) component  $I$ ; (b) component  $Q$

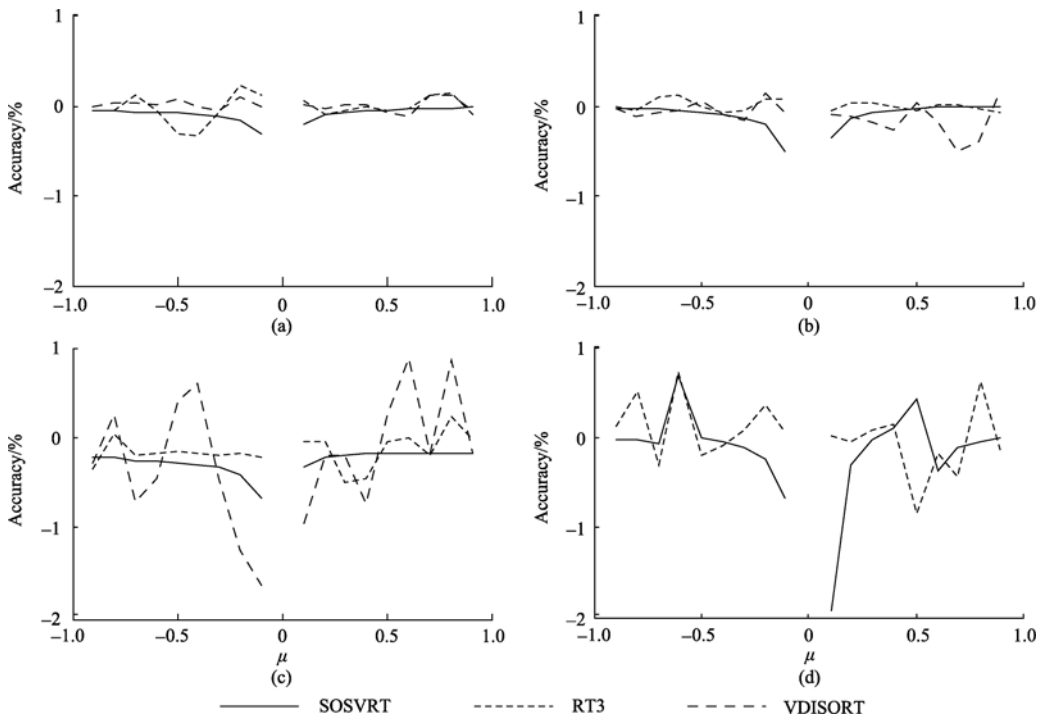


Fig. 2 Error when the azimuth is equal to  $90^\circ$   
(a) component  $I$ ; (b) component  $Q$ ; (c) component  $U$ ; (d) component  $V$

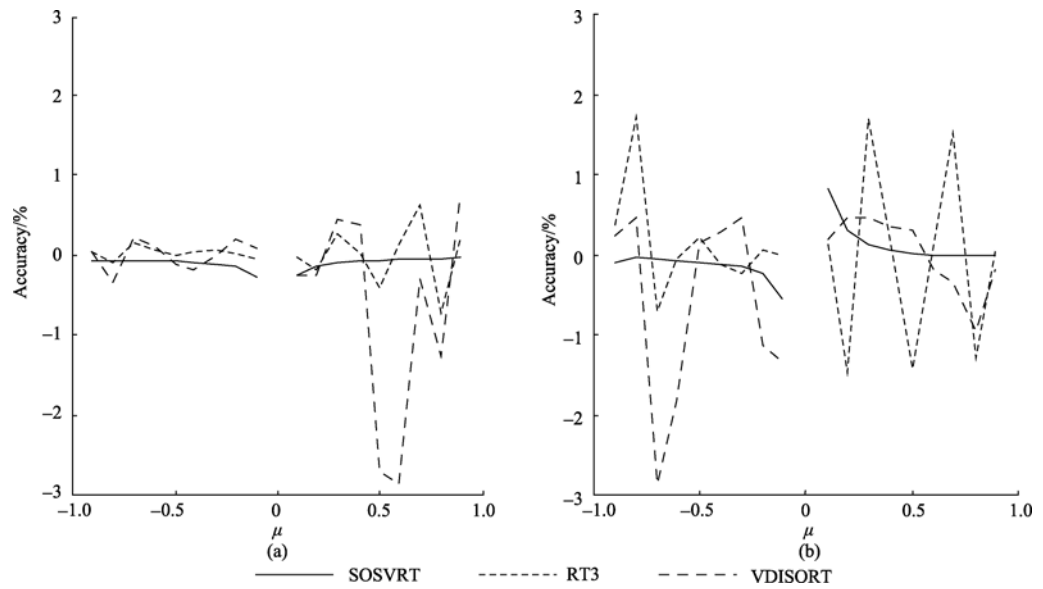


Fig. 3 Error when the azimuth is equal to  $180^\circ$   
(a) component  $I$ ; (b) component  $Q$

### 3.2 Comparison of computing time

The computation time of the three models for different optical depths and streams are compared and tested on the following platform: Windows XP, Quadra-cores CPU of 2.53GHz, memory of 4G, and FORTRAN compiler of Compaq Visual Fortran 6.6c.

#### 3.2.1 Rayleigh scattering

The computation time for a Rayleigh scattering atmosphere is tested under the following condition: cosine of solar zenith angle of 0.6, single scattering albedo of 0.99999, and three azimuth angles of  $0^\circ$ ,  $90^\circ$  and  $180^\circ$ . Only one layer is assumed for the whole atmosphere. The scattering phase matrix can be described as (Hansen & Travis, 1974):

$$P(\alpha) = \begin{bmatrix} \frac{3}{4}(1 + \cos^2 \alpha) & -\frac{3}{4}\sin^2 \alpha & 0 & 0 \\ -\frac{3}{4}\sin^2 \alpha & \frac{3}{4}(1 + \cos^2 \alpha) & 0 & 0 \\ 0 & 0 & \frac{3}{2}\cos \alpha & 0 \\ 0 & 0 & 0 & \frac{3}{2}\cos \alpha \end{bmatrix} \quad (10)$$

The total optical thickness of the Rayleigh scattering atmosphere can be given by (Tang *et al.*, 2006):

$$\tau(\lambda) = 0.00879\lambda^{-4.09}$$

The total Rayleigh optical thickness is 0.57 for a wavelength of 360nm, and 0.37 for 400nm. Only three Legendre coefficients (Eq. (10)) are required for Rayleigh scattering, the streams vary from 4 to 40 in step 4, and the computation time in seconds is illustrated in Fig. 4.

As shown in Fig. 4, the computing time of SOSVRT is the least of the three methods, and increases very slowly with the increase in streams. The time of RT3 is the longest, and increases rapidly with the streams. The computation time of VDISORT also increases with the increasing of the streams, but more weakly than that of RT3.

With fixed streams of 16, the computing time with optical depth is also compared, as illustrated in Fig. 5.

The computing time of SOSVRT increases rapidly with the increasing of the layered optical thickness, while the times of RT3 and VDISORT vary less with optical depth. For fixed 16

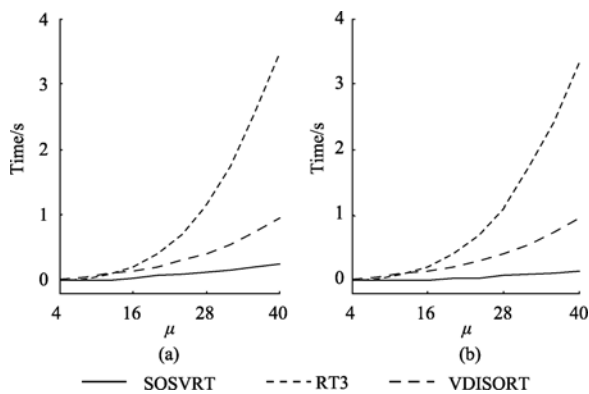


Fig. 4 Seconds vs. stream for a Rayleigh scattering atmosphere (a) 360nm; (b) 400nm

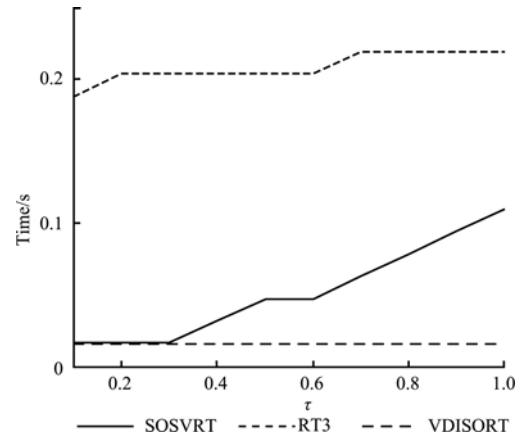


Fig. 5 Seconds vs optical depth. Stream number is set to be 16

streams and an optical depth of 1.0, RT3 spent much more time than SOSVRT, while VDISORT used the least time, less than that of SOSVRT with an optical thickness of 0.1.

#### 3.2.2 Mie scattering conditions

It is assumed that only spheroid particles exist in the atmosphere, the phase function of model 2 in Wauben and Hovenier (1992) is used, as well as a single scattering albedo of 0.973527, and the computation conditions are the same as the case study for Rayleigh scattering.

Variation in computation time with streams at optical depths of 0.5 and 1.0 are shown in Fig. 6:

Similar to that of Rayleigh scattering, the computing time of SOSVRT varies very little with the streams, while it increase greatly with streams for RT3 and VDISORT, especially for large stream numbers. For an optical thickness of 0.5 and 8 streams, the seconds consumed for TR3, VDISORT and SOSVRT are 0.250, 0.312, and 0.125 respectively, while for an optical thickness of 1.0 the values are 2.141, 1.469 and 0.453 s, respectively.

The time-consumed for fixed streams (24 and 48) and different optical thicknesses are illustrated in Fig. 7.

As shown above, the computation time of VDISORT remains almost constant with the increase in optical thickness, and the time consumed for RT3 also increases very slowly with an increase in optical thickness. SOSVRT requires a rapidly increasing time as the optical thickness increases. VDISORT is coded with the inverse of matrix solution, which is not related

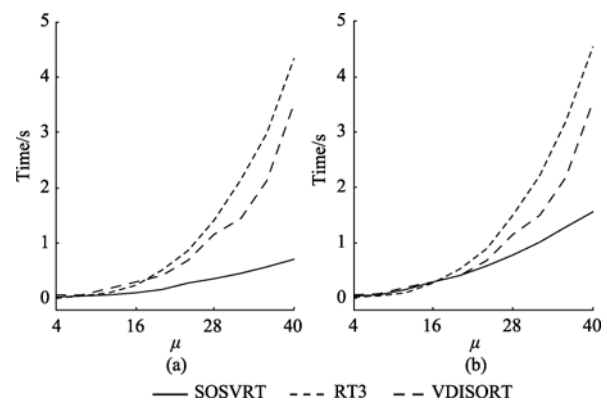


Fig. 6 Seconds vs streams for Mie scattering conditions (a) = 0.5; (b) = 1.0

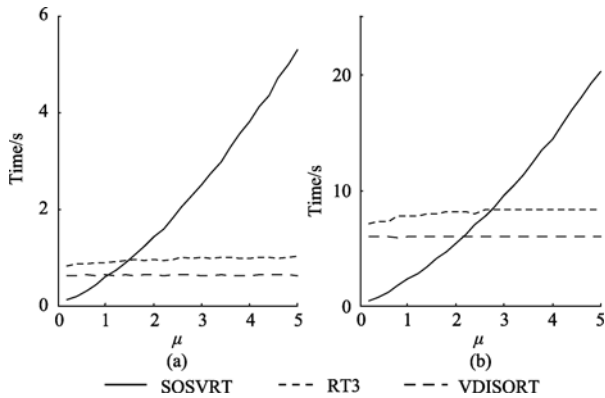


Fig. 7 Seconds vs optical depth for fixed streams  
(a) 24 streams; (b) 48 streams

with the optical depth, and RT3 uses the doubling method for homogeneous layers and only a little time is needed when the optical thickness increases. SOSVRT needs the vertical integration with optical depth, of which the integration step must be small enough to ensure the accuracy, and therefore the time consumed by SOSVRT increases rapidly with an increase in optical depth. Fortunately, the simulations of polarization often apply for clear and thin cirrus sky conditions, of which the optical depth is small. For optically-thick sky conditions, simulation of polarization is not necessary due to the strong depolarization of multiple scattering. Therefore, the SOSVRT code is the most efficient tool in the simulation of polarization.

#### 4 CONCLUSION

Both the accuracy and efficiency of the three polarized models, SOSVRT code based on the SOS method, RT3 code based on the adding-doubling method, and VDISORT code based on the discrete ordinate method, have been compared under Rayleigh and Mie scattering sky conditions. For component *I*, the results for SOSVRT and RT3 were close to the benchmark, and SOSVRT was also stable. Results for RT3 showed small oscillations with zenith angle. At some zenith angles, the results for VDISORT showed large difference, e.g. over 3% for some downward radiation, which may be related to the matrix inversion method. For *Q*, *U*, and *V*, SOSVRT was the most accurate, with the differences less than 0.5%, except in the horizontal direction. The results for RT3 and VDISORT showed oscillation with the zenith angle.

The efficiencies of the three models were compared and tested. For fixed optical depths, the time consumed by RT3 and VDISORT increased greatly, almost exponentially, with the increase in stream number. However, RT3 was much lower than VDISORT. SOSVRT was found to be highly efficient, and the time for SOSVRT increased very slowly as the stream number increased. For 16 streams and an optical thickness of 0.5 in each layer, the seconds consumed for RT3, VDISORT and SOSVRT were 2.141, 1.469 and 0.453s, respectively. For a fixed stream, the time used by RT3 and VDISORT remained almost constant as the optical thickness increased, while the time consumed linearly increased with optical depth for SOSVRT. This explains why the SOS method is less efficient in radiative transfer modeling. However, for thin optical layers,

such as clear and thin cirrus skies, SOSVRT is also one of the most efficient polarized radiative transfer models.

#### REFERENCES

- Chandrasekhar S. 1950. Radiative Transfer. UK: Oxford University Press
- Deuzé J L, Bréon F M, Deschamps P Y, Devaux C, Herman M, Podaire A and Roujean J L. 1993. Analysis of the POLDER (polarization and directionality of earth's reflectance) airborne instrument observations over land surfaces. *Remote Science Environment*, **45**: 137—154
- Duan M Z and Lu D R. 2007. Simultaneously retrieving aerosol optical depth and surface albedo over land from polder's multi-angle polarized measurements: I, theory and simulations. *Chinese Journal of Atmospheric Science*, **31**: 757—765
- Duan M Z and Lu D R. 2008. Simultaneously retrieving aerosol optical depth and surface albedo over land from polder's multi-angle polarized measurements: II, a Case Study. *Chinese Journal of Atmospheric Science*, **32**: 27—35
- Duan M, Min Q and Lu D. 2010. A polarized radiative transfer model based on successive order of scattering. *Adv. Atmos. Sci.*, Doi: 10.1007/s00376-009-9049-8
- Evans K F and Stephens G L. 1991. A new polarized atmospheric radiative transfer model. *Journal of Quantitative Spectroscopy & Radiative Transfer*, **46**(5): 413—423
- Hansen J E and Travis L D. 1974. Light scattering in planetary atmospheres. *Space Science Reviews*, **16**: 527—610
- Lacis A A, Mishchenko C J and Cairns M I. 1998. Modeling errors in diffuse-sky radiation: Vector vs. scalar treatment. *Geophysical Research Letters*, **25**(2): 135—138
- Liou K N and Takano Y. 1994. Light scattering by nonspherical particles: remote sensing and climatic implications. *Atmospheric Research*, **31**: 271—298
- McLinden C A, McConnell J C, Griffioen E and McElroy C T. 2002. A vector radiative-transfer model for the Odin/OSIRIS project. *Canadian Journal of Physics*, **80**: 375—393
- Min Q L and Duan M Z. 2004. A successive order of scattering model for solving vector radiative transfer in the atmosphere. *Journal of Quantitative Spectroscopy & Radiative Transfer*, **87**: 243—259
- Mishchenko M I. 1993. Light scattering by size-shape distributions of randomly oriented axially symmetric particles of a size comparable to a wavelength. *Applied Optics*, **32**: 4652—4665
- Schulz F M, Stammes K and Weng F Z. 1999. VDISORT: an improved and generalized discrete ordinate method for polarized (vector) radiative transfer. *Journal of Quantitative Spectroscopy & Radiative Transfer*, **61**: 105—122
- Shi G Y. 2007. Atmospheric Radiation. Beijing: Science Press
- Siewert C E. 2000. A discrete-ordinates solution for radiative-transfer models that include polarization effects. *Journal of Quantitative Spectroscopy & Radiative Transfer*, **64**: 227—254
- Stam D M and Hovenier J W. 2005. Errors in calculated planetary phase functions and albedos due to neglecting polarization. *Astronomy and Astrophysics*, **444**(1): 275—286
- Tang J K, Xue Y, Yu T, Guan Y N, Cai G Y and Hu Y C. 2006. Aerosol retrieval over land by exploiting the synergy of TERRA and AQUA MODIS DATA. *Science in China: Series D Earth Sciences*, **49**(6): 641—649
- Wauben W M and Hovenier J W. 1992. Polarized radiation of an atmosphere containing randomly-oriented spheroids. *Journal of Quantitative Spectroscopy and Radiative Transfer*, **47**: 491—504
- Weng F Z. 1992. A multi-layer discrete-ordinate method for vector radiative transfer in a vertically-inhomogeneous, emitting and scattering atmosphere—I. theory. *Journal of Quantitative Spectroscopy & Radiative Transfer*, **47**: 19—33

# 典型矢量辐射传输模式计算精度与效率的初步比较

高 扬<sup>1</sup>, 段民征<sup>2</sup>, 黄兴友<sup>1</sup>

1. 南京信息工程大学 大气物理学院, 江苏 南京 210044;

2. 中国科学院 大气物理研究所, 北京 100029

**摘 要:** 辐射传输模式是建立遥感反演方法和气候模式中辐射参数化的重要工具, 尤其是全偏振的矢量辐射传输模式对于精确理解地气系统中的辐射过程至关重要。PolRadtran/RT3(polarized radiative transfer)、SOSVRT (vector radiative transfer based on successive order of scattering)和 VDISORT(vector DIScrete ordinate radiative transfer)是基于不同物理原理求解矢量辐射传输的三个代表性数值模式。对这三个模式进行计算时间和计算精度的比较, 发现, 基于逐次散射法的 SOSVRT 计算效率最高, 计算时间基本不随流数的增加而增长, 但随单层光学厚度的增大, 其计算时间有较为明显的增加, 在米散射情况下, 光学厚度从 0.5 增加到 1.0 时, 其计算时间增加了 1 倍; 基于倍加累加法的 RT3 和基于矩阵特征矢量求解方法的 VDISORT 计算效率较低, 尤其是采用大流数计算时, RT3 和 VDISORT 的计算时间随流数的增加迅速增长, 特别是在瑞利散射条件下, 波长为 400nm, 流数为 40 时, 其计算时间分别为 SOSVRT 的 23 倍和 7 倍。但是, 两模式随光学厚度增加计算时间却无明显的增加。在计算精度方面, 3 个模式比较接近, 只是 VDISORT 在大流数的情况下会有震荡现象。

**关键词:** 矢量辐射传输, 倍加累加法, 逐次散射法, 离散坐标法

中图分类号: TP701

文献标志码: A

**引用格式:** 高 扬, 段民征, 黄兴友. 2010. 典型矢量辐射传输模式计算精度与效率的初步比较. 遥感学报, 14(5): 839—851  
Gao Y, Duan M Z and Huang X Y. 2010. Preliminary comparisons of the typical polarized radiative transfer models: precision and efficiency. *Journal of Remote Sensing*. 14(5): 839—851

## 1 引 言

辐射测量及其在大气中的传输过程模拟是大气遥感的重要手段之一, 在准确进行辐射传输计算时, 不仅要考虑辐射强度或通量, 也要考虑辐射的偏振状态。研究表明如果忽略偏振因素, 在进行行星大气的散射强度和辐射通量的计算时会造成约为 10% 的误差(Chandrasekhar, 1950); Lacis 等(1998)指出, 标量辐射传输模式在本质上是不完善的, 不能胜任高精度的计算和分析, 在清洁大气情况下, 利用标量辐射传输模式计算辐射强度的误差为 5%—10%; Stam 和 Hovenier(2005)指出, 不考虑偏振带来的误差会对利用气体吸收带反演成分混合比和粒子形状产生明显的影响, 误差会达到 10%以上、甚至更大。

由于偏振辐射信号可以区分大气与地表对总的行星反照的贡献(Deuzé 等, 1993; 段民征 & 吕达仁,

2007, 2008), 可以区分水云和冰云(Liou & Takano, 1994), 还可以确定散射粒子的形状(Mishchenko, 1993)。因此, 偏振探测手段越来越受到大气和天文学研究工作者的关注, 如法国 CIMEL 公司的 CE-318 地基太阳光度计, 星载的 POLDER 系列传感器, 以及 2010 年将要发射的 GLORY 卫星上搭载的气溶胶偏振传感器(APS)等, 如果没有相应完备的矢量辐射传输模式, 偏振辐射的测量数据就不能被很好的利用, 由于偏振分量比较小, 特别是 V 分量, 其量级一般只有  $10^{-4}$ — $10^{-5}$ , 所以要求矢量辐射传输模式要有很高的计算精度, 另外, 相对于标量辐射传输模式, 矢量辐射传输模式虽然能更好的描述大气的真实情况, 但其计算时间会更长, 所以, 在对偏振辐射测量值进行反演时, 就需要选择一种计算速度快并且计算精度高的矢量辐射传输模式。目前, 应用和发展比较完善的矢量辐射传输有 Evans(1991)等发展的基于倍加累

收稿日期: 2009-11-10; 修订日期: 2010-04-28

基金项目: 国家高技术研究发展计划(编号: 2009AA12Z151), 国家重点基础研究发展计划(编号: 2006CB403702)资助和国家重点基础研究发展计划(编号: 2006CD403707)。

第一作者简介: 高扬(1985—), 男, 硕士研究生, 南京信息工程大学, 从事气溶胶辐射效应方面研究。E-mail: tony0519@sohu.com。

加法原理的 PolRadtran/RT3(polarized radiative transfer) (以下简称 RT3), Schulz 等(1999)在 Stamnes 等的标量离散坐标法 DISORT 模式的基础上发展的矢量模式 VDISORT(vector discrete ordinate radiative transfer), 以及基于逐次散射法的 SOSVRT(vector radiative transfer based on successive order of scattering)(Min & Duan, 2004; Duan 等, 2010)全矢量大气辐射传输模式。

## 2 矢量辐射传输方程

辐射能量及其偏振状态可以用 Stokes 矢量  $I = [I, Q, U, V]^T$  来描述, 其中  $I$  代表总的辐射强度,  $Q$  代表辐射场矢量端点轨迹类型,  $U$  表示椭圆长轴取向,  $V$  表示偏振矢端旋转方向(McLinden 等, 2002), 上标 T 是转置矩阵的标志, 当只考虑  $I$  分量时, 为一般的标量辐射传输方程, 矢量辐射传输方程在平面平行吸收散射介质中的传播和分布可以表示为:

$$\mu \frac{dI(\tau, \mu, \phi)}{d\tau} = -I(\tau, \mu, \phi) + J(\tau, \mu, \phi) \quad (1)$$

其中源函数  $J(\tau, \mu, \phi)$  可写为:

$$J(\tau, \mu, \phi) = \frac{\omega}{4\pi} \int_0^{2\pi} \int_{-1}^1 M(\tau, \mu, \phi; \mu', \phi') I(\tau, \mu', \phi') d\mu' d\phi' + \frac{\omega}{4\pi} F_0 \exp(-\tau/\mu_0) M(\tau, \mu, \phi; -\mu_0, \phi_0) \quad (2)$$

$$I = \sum_{m=0}^M [I_m \cos m(\phi - \phi_0), Q_m \cos m(\phi - \phi_0), U_m \sin m(\phi - \phi_0), V_m \sin m(\phi - \phi_0)]^T \quad (6)$$

$$M = \frac{1}{2} C_0 + \sum_{m=1}^M [C_m \cos m(\phi - \phi') + S_m \sin m(\phi - \phi')] \quad (7)$$

其中  $C_m$  和  $S_m$  为第  $m$  次傅里叶模态的系数。式(1)可改写为(Duan 等, 2009):

$$\mu \frac{dI_m(\tau, \mu)}{d\tau} = -I_m(\tau, \mu) + J_m(\tau, \mu) \quad (8)$$

其中  $J_m$  为:

$$J_m(\tau, \mu) = \frac{\omega}{4} \int_{-1}^1 M_m(\tau, \mu; \mu') I_m(\tau, \mu) d\mu' + \frac{(2 - \delta_{0m}) \omega}{2} \frac{\omega}{4\pi} \exp(-\tau/\mu_0) M_m(\tau, \mu; -\mu_0) F_0 \quad (9)$$

在对上述辐射传输方程进行数值求解过程中, 首先是对辐射传输方程进行离散化, 基于不同离散化形式和求解过程派生出多种辐射传输模式。下面将针对目前常用的 3 种矢量辐射传输模式的计算效率和计算精度进行对比分析。

### 2.1 倍加累加法

倍加累加法是基于直观物理过程得到的一种方法, 它应用于平面平行、垂直不均匀散射大气的偏

$\mu$  为天顶角余弦值, 通常规定向下为正、向上为负。 $\phi$  相对于太阳光束的方向角。 $\tau$  为光学厚度,  $\omega$  是单次散射反照率,  $F_0 = [F_0, 0, 0, 0]$ ,  $F_0$  为太阳入射能流,  $\mu_0$  和  $\phi_0$  分别是天顶角和方向角的余弦值。式(2)中, 右边的第一项是多次散射的贡献项, 第二项是对来自上一层边界的入射辐射所造成的单次散射的贡献项,  $M$  为  $4 \times 4$  阶散射相矩阵, 又称 Mueller 矩阵, 它是通过单次散射相矩阵  $P$  经参考平面旋转变换后得到的, 它的转换公式可表示为:

$$M = L(\pi - i_2) P L(-i_1) \quad (3)$$

其中:

$$L(i) = \begin{bmatrix} 1 & 0 & 0 & 0 \\ 0 & \cos 2i & \sin 2i & 0 \\ 0 & -\sin 2i & \cos 2i & 0 \\ 0 & 0 & 0 & 1 \end{bmatrix} \quad (4)$$

一般的, 对于球形和镜面对称的随机取向的散射粒子而言,  $P$  可以写为:

$$P = \begin{bmatrix} a_1 & b_1 & 0 & 0 \\ b_1 & a_2 & 0 & 0 \\ 0 & 0 & a_3 & b_2 \\ 0 & 0 & -b_2 & a_4 \end{bmatrix} \quad (5)$$

为求解简单并考虑数值求解的稳定性, 通常使用傅里叶变换对其进行分解, STOKES 矢量  $I$  和散射相函数  $M$  的傅里叶展开形式可表述为:

振辐射传输方程的计算。其原理为: 如果两个气层的反射状态和透射状态是已知的, 那么这两个层所组成的合层的反射状态和透射状态可以通过简单的累加方式得到, 依此类推就可计算整层大气的反射矩阵和透射矩阵, 并将边界作为一层来处理, 从而可以求得大气顶向上和地表向下的矢量辐射。

在倍加累加法中, 对于一个厚的均匀层, 将其划分为  $2^N$  个完全相同的薄层, 通过倍加法可计算出整个层结的反射和透射函数, 大大加快计算速度。倍加法用来求均匀层结的反射透射矩阵, 而非均匀层之间采用累加法。在应用这种算法的 RT3 模式中, 方位的展开是以 Fourier 级数形式给出, 并对天顶角进行离散化。模式中包括了两种地表类型: 朗伯型和费涅尔型。利用倍加累加法计算大气层的多次散射时, 不仅易于理解, 而且计算稳定(Evans & Stephens, 1991)。

### 2.2 逐次散射法

逐次散射法(the successive order of scattering

method, SOS)是计算逐次散射最直接的近似方法。在逐次散射法中,先分别计算 1 次、2 次、3 次、...、 $N$  次散射的强度,再对各次散射强度进行求和得到总散射强度(Min & Duan, 2004)。

逐次散射法矢量辐射传输算法的精度受垂直分层数和流数的影响,也和散射次数有关。如果每一个垂直分层的厚度很小,并且选用大流数进行计算,那么,其精度会很高,但这是以牺牲计算速度为代价的。

为了计算任意角度的 Stokes 矢量和给定积分角与垂直层的厚度,在 SOSVRT 算法中,采用角度内插法处理源函数,这种方法比采用标准内插法更为精确。

对于前向散射很强的介质,采用低阶多项式近似的办法,不能正确反映方向差异性很强的相函数,并易引起解的震荡,而高阶多项式近似使计算时间成倍增长。为提高计算效率并抑制虚假震荡, SOSVRT 中引入了  $\delta$ -M 方法,这个处理方案已被证明了其对强各项异性散射介质的处理是最有效的。

与其他方法相比,逐次散射法能够有效地处理散射-吸收过程。当用逐次散射法计算光子的散射时,介质非均匀性和气体吸收的影响也得到了体现。也就是说,逐次散射法也适用于不均匀大气的情况。此外,逐次散射法也可用于遥感的快速计算和全球气候模式中辐射传输过程的参数化处理。逐次散射法的缺点之一是在进行强度收敛的计算时需要加大计算量,在处理光学厚度大或单次散射反照率较大的介质时,计算量的增加尤为突出。但是,大多数情况下,气溶胶和卷云的偏振影响是比较小的。并且,由于对算法进行了一些优化,所以在精度相同的情况下,计算时间可以大大减少。因此,求解大气辐射传输的偏振特性,逐次散射法比其他算法有较大的优势。

### 2.3 离散坐标法

离散坐标法是将辐射传输方程(8)和(9)离散化,转化为具有  $2n$  个方程( $2n$  为离散化角度的个数)的一阶线性微分方程组。然后通过求解本征矩阵特征值和特征矢量的方法获得矢量辐射传输方程的解,在对特征矩阵求解时, VDISORT 应用了矩阵求逆的方法。当  $n=1$  时,即为我们所熟悉的二流近似(石广玉, 2007),即有一个向上的流和一个向下的流。但当流数很大时,其特征矩阵会变得比较松散,在对这样的特征矩阵进行矩阵求逆后,其特征值和特征矩阵会出现异常,导致最后的结果出现震荡。

离散坐标法的特点是它可以给出反射和透射过

程的内部变化,对于计算散射强度和通量既有效又准确(Weng, 1992)。因此,在计算气溶胶和有云大气的辐射场时,是一种有效的方法。

通过以上介绍,我们可以发现, VDISORT 是基于对辐射传输方程直接进行离散化处理,而 RT3 和 SOSVRT 这两种模式都是基于物理过程而实现对辐射传输方程的求解。在计算气溶胶和卷云的偏振辐射时,要求矢量辐射传输模式具有很高的计算效率和计算精度,由于光学厚度和流数是影响矢量辐射传输模式的两个很重要的物理量。所以选用这 2 个量作为对 3 个模式进行比较的指标。

## 3 模式比较

在瑞利散射和米散射两种情形下,对以上 3 个通用的矢量辐射传输模式进行计算效果比较。计算中,散射相函数在 RT3 中应用了 Legendre 展开函数,而在 SOSVRT 和 VDISORT 中应用了通用的球谐展开函数,具体的展开方法参见文献(Hansen 和 Travis), (1974)。

### 3.1 计算精度的比较

首先进行 3 种模式的计算精度比较,假定大气为一层散射均匀介质,光学厚度为 1,单次散射反照率为 0.973527,散射相函数由长短轴比为 1.999987,折射率为  $1.53-0.006i$  的椭球粒子,具体参见文献(Wauben 和 Hovenier), (1992)中的模型 2。太阳天顶角的余弦取 0.6,半球流数为 16,方位角相对于太阳光线方向分别取  $0^\circ$ ,  $90^\circ$  和  $180^\circ$ ,不考虑地表反射。

图 1—图 3 给出了相同计算条件下 3 种模式计算结果的误差比较,参考值取 Wauben 和 Hovenier (1992)文献中数值表,他们的结果经过了多种模式的严格验证,精度为 7 位有效数字,是验证矢量辐射传输模式(Siewert, 2000; Duan 等, 2004, 2008)的参考基准。由于 RT3 和 VDISORT 采用样条插值方法求取给定观测方向的辐射值,所以,在天顶(-1)和天底(1),采用外推得到结果误差较大,可能高达 20% 以上,前向散射的误差也较大,而在其他利用内插处理的观测方向(前向散射除外),误差基本在 1% 以内。SOSVRT 模式中采用了源函数分析式的差分方法,所以,在所有角度上误差均较小。对于  $I$  分量, SOSVRT 和 RT3 两个模式的计算结果和标准值均很接近,误差在 1% 以内。VDISORT 计算的大部分结果比较接近参考值,但在背向太阳方向,  $I$  分量出现了较大误差。除天顶和天底两个方向外,在 0.6 附近的地面向下辐射也出现了大于 3% 的较大误差。

对于其他 3 个分量( $Q, U, V$ ), SOSVRT 的结果与标准值最为接近, 除水平方向外(天顶角大于  $80^\circ$  时平面平行模式不适用), 误差均在 0.5% 以内; 而 RT3 和 VDISORT 的误差, 随角度分布出现明显震荡, 尤其是 VDISORT 模式的  $V$  分量计算误差极大, 通常可达 100% 以上。

### 3.2 计算时间的比较

我们还比较分析了 3 种模式在给定单层光学厚

度条件下计算时间随流数的变化, 以及给定计算流数情况下, 计算时间随单层光学厚度的变化。所采用的计算环境为: Windows XP, 4 核 2.53GHz CPU, 内存 4G, Compaq Visual Fortran 6.6c 编译器。

#### 3.2.1 瑞利散射情况

在瑞利散射假设下进行计算时间的比较时, 假设大气为单层, 其初始天顶角的余弦值为 0.6, 方位角取  $0^\circ, 90^\circ$  和  $180^\circ$ 。单次散射反照率为 0.99999, 散射相矩阵的形式为(Hansen & Travis, 1974):

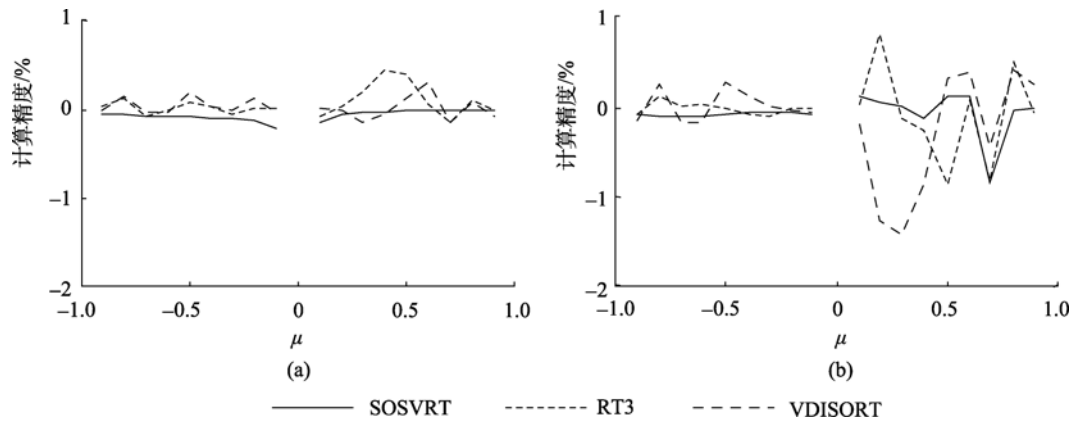


图 1 方位角为  $0^\circ$  时误差分析  
(a)  $I$  分量; (b)  $Q$  分量的误差

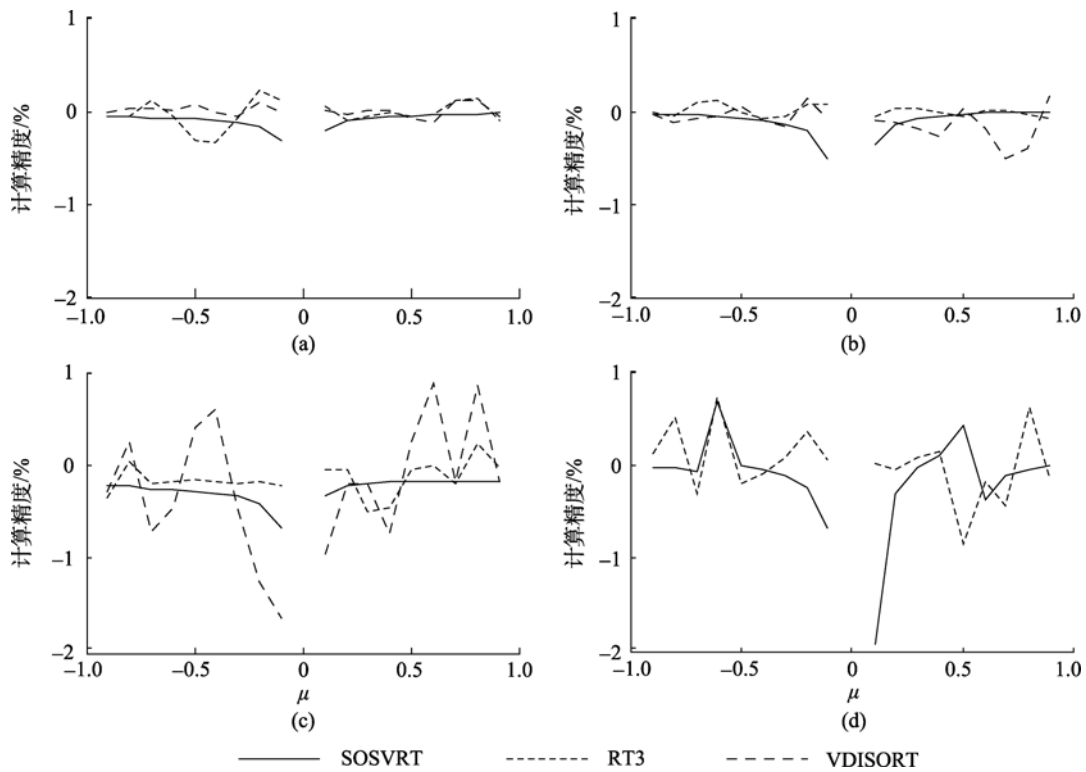


图 2 方向角为  $90^\circ$  时的误差  
(a)  $I$  分量; (b)  $Q$  分量; (c)  $U$  分量; (d)  $V$  分量

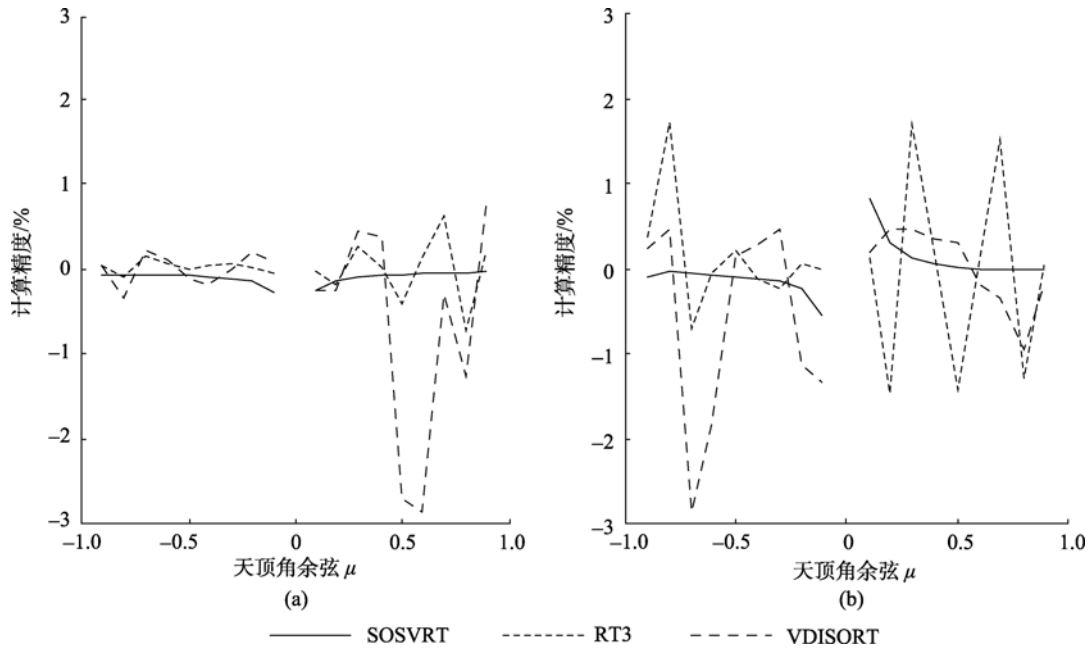


图 3 方位角为 180°时误差分析  
(a) I 分量; (b) Q 分量

$$P(\alpha) = \begin{bmatrix} \frac{3}{4}(1 + \cos^2 \alpha) & -\frac{3}{4}\sin^2 \alpha & 0 & 0 \\ -\frac{3}{4}\sin^2 \alpha & \frac{3}{4}(1 + \cos^2 \alpha) & 0 & 0 \\ 0 & 0 & \frac{3}{2}\cos \alpha & 0 \\ 0 & 0 & 0 & \frac{3}{2}\cos \alpha \end{bmatrix} \quad (10)$$

瑞利散射的光学厚度可根据下式得到(Tang 等, 2006):

$$\tau(\lambda) = 0.00879\lambda^{-4.09}$$

所以波长为 360nm 的光学厚度为 0.57, 波长为 400nm 的光学厚度为 0.37。对公式(10), 利用勒让德函数展开, 得到三项勒让德展开系数。为了比较计算时间, 取流数为 4—40, 流数步长为 4, 所得的结果如图 4。

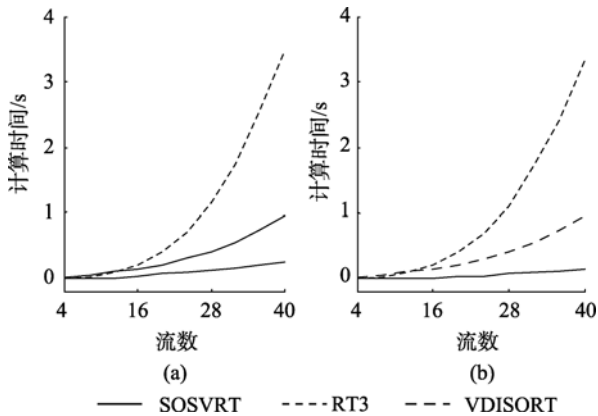


图 4 瑞利散射情况, 不同流数下的计算时间比较  
(a) 360nm; (b) 400nm

从图 4 看出, SOSVRT 所用的计算时间是最少的, 不随流数的变化而发生很大的变化; RT3 所用的计算时间最长, 且随着流数的增加而迅速增加; VDISORT 所用的计算时间随着流数的增加而增加, 和 RT3 相比, VDISORT 没有随着流数的增加而迅速增加。

在 16 流数的情况下, 瑞利散射大气光学厚度的变化对计算时间的影响如图 5。

从图 5 看出, SOSVRT 的计算时间随着光学厚度的增加而明显增加, RT3 和 VDISORT 两个模式的计算时间随光学厚度的变化很小; RT3 的计算时间最长, 超过了 SOSVRT 在光学厚度为 1.0 处所用的计算时间; VDISORT 的计算时间最短, 比 SOSVRT 在

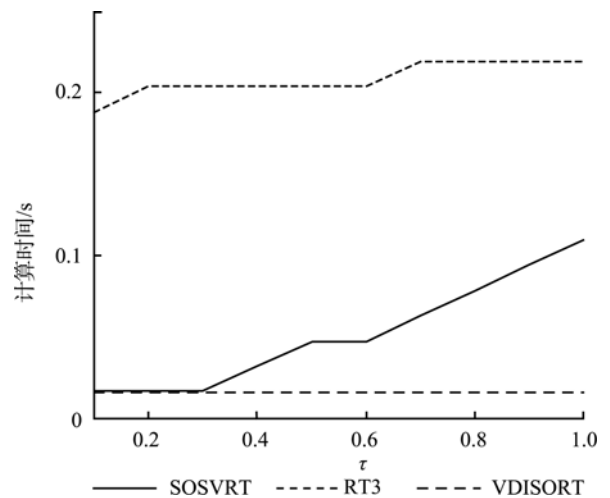


图 5 瑞利散射情况, 计算时间随光学厚度的变化

光学厚度为 0.1 处的计算时间还要短。

### 3.2.2 米散射情况

假定大气只含有椭球型气溶胶粒子, 相函数取文献 Wauben 和 Hovenier(1992)中模型 2 的情况, 单次散射反照率为 0.973527, 其他计算条件与瑞利散射的相同。

先取光学厚度为 0.5 和 1.0 两种情况分析 3 种模式的计算效率, 图 6 给出了计算时间和计算流数的关系:

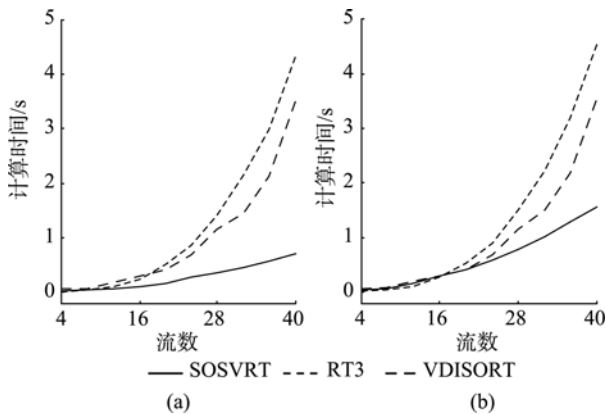


图 6 m 散射下, 不同流数下的计算时间比较  
(a)  $\tau=0.5$ ; (b)  $\tau=1.0$

通过图 6 看出, 同瑞利散射情况相似, SOSVRT 的计算时间并没有随着流数的增加而发生明显的变化, RT3 和 VDISORT 的计算时间随着流数的增加明显增加, 尤其是采用大流数计算时, 如单层光学厚度为 0.5 时, 流数为 8 时, RT3, VDISORT, SOSVRT 所用时间分别为 0.250, 0.312 和 0.125s, 如单层光学厚度为 0.5 时, 流数为 16 时, RT3, VDISORT, SOSVRT 所用时间分别为 2.141, 1.469 和 0.453s。

图 7 给出了计算时间随单层光学厚度的变化情况, 流数分别为 24 和 48 流:

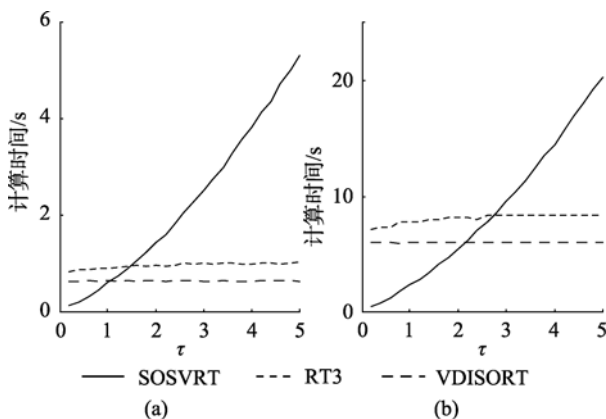


图 7 m 散射下, 计算时间随光学厚度的变化  
(a) 流数=24; (b) 流数=48

从图 7 看出, VDISORT 的计算时间基本不随单层光学厚度的变化而变化, RT3 的计算时间随着光学厚度的变化很小, 而 SOSVRT 的计算时间随着光学厚度的增加而增加。这是因为 VDISORT 是矩阵求解过程, 与单层光学厚度无关, RT3 对于均匀介质层采用了倍加处理方法, 光学厚度有限增加, 计算时间增加很少, 而 SOSVRT 方法因采用垂直积分, 与光学厚度大小有直接关系。但是, 在利用矢量辐射传输模式模拟大气辐射传输过程时, 通常只考虑晴空或薄云大气, 光学厚度一般较小。而对于光学厚度较大的天气条件, 由于强多次散射的消偏, 偏振模拟已经不重要。因此, SOSVRT 依然是计算效率最好的模拟工具。

## 4 结 论

本文对基于逐次散射法的 SOSVRT、基于倍加累加法的 RT3 和基于逆矩阵求解的 VDISORT 3 个矢量辐射传输模式的计算效能进行了比较分析, 分别比较了在瑞利散射和米散射大气条件下, 3 种模式的计算精度和计算效率。结果表明, 对于  $I$  分量, SOSVRT 与 RT3 的计算结果与参考值接近, SOSVRT 模式计算结果平稳, 而 RT3 模式的结果随角度分布出现小幅震荡。VDISORT 模式在某些方向的计算误差较大, 可能与其矩阵求逆有关, 对于地面向下辐射, 有些角度的误差超过了 3%。对于  $(Q, U, V)$  3 个分量, SOSVRT 精度最好, 除水平方向外, 误差均在 0.5% 以内, 而 RT3 和 VDISORT 的误差, 随角度出现明显震荡, 计算不平稳。

同时, 我们还对 3 个模式的计算效率进行了比较分析。在光学厚度一定时, RT3 和 VDISORT 模式随流数的增加, 计算时间几乎呈指数增加, 其中 RT3 计算效率更低。SOSVRT 模式的计算时间随流数的增加而缓慢增长, 计算效率较高。在单层光学厚度 0.5、流数为 16 时, RT3, VDISORT 和 SOSVRT 所用计算时间分别为 2.141, 1.469 和 0.453s。在流数给定时, RT3 和 VDISORT 的计算时间基本上不随单层光学厚度的变化而变化, SOSVRT 的计算时间随单层光学厚度的增加而呈线性增长, 这也是普遍认为逐次散射法效率低的原因。但是, 在较小的单层光学厚度时, 如晴空大气或是薄卷云, SOSVRT 模式依然是计算效率最高的矢量辐射传输模式。

## REFERENCES

Chandrasekhar S. 1950. Radiative Transfer. UK: Oxford University

- Press
- Deuzé J L, Bréon F M, Deschamps P Y, Devaux C, Herman M, Podaire A and Roujean J L. 1993. Analysis of the POLDER (polarization and directionality of earth's reflectance) airborne instrument observations over land surfaces. *Remote Science Environment*, **45**: 137—154
- Duan M Z and Lu D R. 2007. Simultaneously retrieving aerosol optical depth and surface albedo over land from polder's multi-angle polarized measurements: I, theory and simulations. *Chinese Journal of Atmospheric Science*, **31**: 757—765
- Duan M Z and Lu D R. 2008. Simultaneously retrieving aerosol optical depth and surface albedo over land from polder's multi-angle polarized measurements: II, a Case Study. *Chinese Journal of Atmospheric Science*, **32**: 27—35
- Duan M, Min Q and Lu D. 2010. A polarized radiative transfer model based on successive order of scattering. *Adv. Atmos. Sci.*, Doi: 10.1007/s00376-009-9049-8
- Evans K F and Stephens G L. 1991. A new polarized atmospheric radiative transfer model. *Journal of Quantitative Spectroscopy & Radiative Transfer*, **46**(5): 413—423
- Hansen J E and Travis L D. 1974. Light scattering in planetary atmospheres. *Space Science Reviews*, **16**: 527—610
- Lacis A A, Mishchenko C J and Cairns M I. 1998. Modeling errors in diffuse-sky radiation : Vector vs.scalar treatment. *Geophysical Research Letters*, **25**(2): 135—138
- Liou K N and Takano Y. 1994. Light scattering by nonspherical particles: remote sensing and climatic implications. *Atmospheric Research*, **31**: 271—298
- McLinden C A, McConnell J C, Griffioen E and McElroy C T. 2002. A vector radiative-transfer model for the Odin/OSIRIS project. *Canadian Journal of Physics*, **80**: 375—393
- Min Q L and Duan M Z. 2004. A successive order of scattering model for solving vector radiative transfer in the atmosphere. *Journal of Quantitative Spectroscopy & Radiative Transfer*, **87**: 243—259
- Mishchenko M I. 1993. Light scattering by size-shape distributions of randomly oriented axially symmetric particles of a size comparable to a wavelength. *Applied Optics*, **32**: 4652—4665
- Schulz F M, Stamnes K and Weng F Z. 1999. VDISORT: an improved and generalized discrete ordinate method for polarized (vector) radiative transfer. *Journal of Quantitative Spectroscopy & Radiative Transfer*, **61**: 105—122
- Shi G Y. 2007. Atmospheric Radiation. Beijing: Science Press
- Siewert C E. 2000. A discrete-ordinates solution for radiative-transfer models that include polarization effects. *Journal of Quantitative Spectroscopy & Radiative Transfer*, **64**: 227—254
- Stam D M and Hovenier J W. 2005. Errors in calculated planetary phase functions and albedos due to neglecting polarization. *Astronomy and Astrophysics*, **444**(1): 275—286
- Tang J K, Xue Y, Yu T, Guan Y N, Cai G Y and Hu Y C. 2006. Aerosol retrieval over land by exploiting the synergy of TERRA and AQUA MODIS Data. *Science in China: Series D Earth Sciences*, **49**(6): 641—649
- Wauben W M and Hovenier J W. 1992. Polarized radiation of an atmosphere containing randomly-oriented spheroids. *Journal of Quantitative Spectroscopy and Radiative Transfer*, **47**: 491—504
- Weng F Z. 1992. A multi-layer discrete-ordinate method for vector radiative transfer in a vertically-inhomogeneous, emitting and scattering atmosphere—I. theory. *Journal of Quantitative Spectroscopy & Radiative Transfer*, **47**: 19—33

#### 附中文参考文献

- 段民征, 吕达仁. 2007. 利用多角度 POLDER 偏振资料实现陆地上空大气气溶胶和地表反照率的同时反演——理论与模拟. *大气科学*, **31**, 757—765
- 段民征, 吕达仁. 2008. 利用多角度 POLDER 偏振资料实现陆地上空大气气溶胶和地表反照率的同时反演——实例分析. *大气科学*, **32**, 27—35
- 石广玉. 2007. 大气辐射学. 北京: 科学出版社